Epitaxial interactions between molecular overlayers and ordered substrates

Andrew C. Hillier* and Michael D. Ward†
Department of Chemical Engineering and Materials Science, University of Minnesota, Amundson Hall, 421 Washington Avenue Southeast, Minneapolis, Minnesota 55455
(Received 13 May 1996)

A framework for evaluating the epitaxy of crystalline organic overlayers of generic symmetry on ordered substrates is described, which combines a computationally efficient analytical method for explicit determination of the type of epitaxy (i.e., commensurism, coincidence, or incommensurism) and overlayer azimuthal orientation with an analysis of the elastic properties of the overlayer and the overlayer-substrate interface. The azimuthal orientations predicted by the analytical method agree with values predicted by semiempirical potential-energy calculations and observed experimentally for previously reported organic overlayers which are demonstrated here to be coincident. Calculations based on this analytical approach are much less computationally intensive than potential-energy calculations, as the number of computational operations is independent of the overlayer size chosen for analysis. This enables analyses to be performed for the large overlayer basis sets common for molecular overlayers. Furthermore, this facilitates the analysis of coincident overlayers, for which the overlayer size needs to be large enough to establish a phasing relationship between a substrate and a large nonprimitive overlayer supercell so that the global minimum with respect to azimuthal angle can be determined. The computational efficiency of this method also enables a convenient examination of numerous possible reconstructed overlayer configurations in which the lattice parameters are bracketed around those of the native overlayer, thereby allowing examination of possible epitaxy-driven overlayer reconstructions. When combined with calculated intralayer- and overlayer-substrate elastic constants, this method provides a strategy for the design of heteroepitaxial molecular films. [S0163-1829(96)01343-4]

INTRODUCTION

The fabrication of molecular thin films with highly ordered, crystalline structures has received considerable attention in attempts to develop materials for molecular-based electronic devices, sensors, displays, and logic elements.[1] The interest in molecular films stems primarily from the ability to tailor the electronic and optical properties systematically by judicious choice of molecular constituents. Monolayers and multilayers with redox-active components capable of supporting electronic conduction have been prepared by the attachment of organosulfur and organosilanes to solid surfaces, with functional multilayers built by chemical reactions on these two-dimensional interfaces.[2–4] Epitaxial growth of monolayer and multilayer films of redox-active charge-transfer salts has been accomplished in solution using electrochemical methods.[5] Thin films of organic dyes on van der Waals substrates such as graphite, MoS_2, and SnS_2 have been prepared by molecular-beam-epitaxy methods.[6] Successful fabrication of molecular films with preordained properties hinges on control of several characteristics, including the supramolecular structure of the film, its azimuthal orientation with the respect to the substrate, and the nature and distribution of defects present in the film.

Investigations of the growth of elemental and inorganic thin films,[7] and to a lesser extent molecular films, indicate that film properties can be influenced significantly by interactions between the primary (i.e., initial) overlayer and the substrate upon which it forms. These interactions commonly are associated with overlayer-substrate epitaxy in which the overlayer and substrate lattices are ''in phase,'' so that their interatomic potentials are reinforced. However, the actual structure of an overlayer will reflect a competition between the energy lowering achieved by epitaxy, and the energetic penalty associated with any reconstruction of the overlayer lattice from its native form that may be required in order to achieve that epitaxy. Consequently, the design of thin films must take into account the relative strengths of intermolecular interactions in the primary overlayer and those between the overlayer and substrate.[8] Controlling these factors is imperative, as reconstruction of the primary overlayer from its native form or stress-induced defects can affect the quality of multilayer films and bulk crystals grown from the primary overlayer.

While there have been significant advances in the understanding of the physical and electronic properties of molecular films, there exists a need for paradigms enabling *a priori* the design of heteroepitaxial molecular overlayers. We have been employing a strategy for the design of molecular films in which the native structure of a molecular overlayer, considered to be at or near its minimum-energy configuration, is surmised from its structure in bulk crystals, which generally consist of layered structures stacked in the third dimension by weak van der Waals interactions.[9,10] The tendency of molecules to assemble in the solid state into two-dimensional layers with strong intralayer bonding (e.g., through hydrogen bonding, charge transfer, or heteroatom-heteroatom interactions) suggests that layered motifs in bulk crystals are ideal design elements for the fabrication of heteroepitaxial films on appropriately chosen substrates. This strategy must include methodology for identifying the optimum overlayer structure and its epitaxial relationship with a particular substrate, and for evaluating the energetics of the overlayer and the substrate-overlayer interface. Recent reports have de-

scribed methods for analyzing overlayer-substrate epitaxy which involve calculation of the total potential energy, use of an elliptical potential,[8] or numerical iteration to determine the degree of fit between the overlayer and substrate lattices.[11] However, these methods tend to be computationally intensive when applied to molecular overlayers due to the large basis sets that are required for these systems. In addition, the latter method is somewhat lacking with respect to direct theoretical significance.

Herein we report a simple analytical method for analyzing overlayer-substrate epitaxy that enables rapid determination of optimum epitaxial relationships with respect to overlayer orientation and structure for generic overlayer lattices. This method is computationally efficient because it is independent of overlayer size, and provides an explicit determination of the type of epitaxy; that is, whether the overlayer is commensurate, coincident, or incommensurate. When combined with calculations of overlayer and overlayer-substrate elastic constants for native overlayers whose structures are surmised from either crystal structures, calculations, or experimental data, this approach enables rapid analysis of overlayer-substrate systems and a qualitative assessment of the tendency for overlayer reconstruction from its native form. The method also enables convenient searching for epitaxial relationships between a rigid substrate and many possible reconstructed forms of an overlayer, and suggests that an *a priori* design of overlayer-substrate systems is feasible.

METHODS AND MATERIALS

Molecular overlayers were synthesized from reagent grade materials, with bis(ethylenedithiolo)-tetrathiafulvalene (ET), tetrathiafulvalene (TTF), tetracyanoquinodimethane (TCNQ), and perylene (Pe) obtained from Strem Chemicals, Newburyport, MA. Solvents used for electrodeposited molecular films were HPLC grade. The n-$Bu_4N^+ClO_4^-$ electrolyte was obtained commercially (Aldrich, Milwaukee, WI), and was recrystallized from acetonitrile prior to use. The electrolyte n-$Bu_4N^+I_3^-$ was prepared by a previously reported method[12] in which I_2 was added to a boiling solution of chloroform or water containing excess n-$Bu_4N^+I^-$ (Aldrich, Milwaukee, WI). The black precipitate formed upon mixing was recrystallized twice from methanol to provide dark, lustrous crystals of n-$Bu_4N^+I_3^-$, and the purity was confirmed by elemental analysis. Electrochemical syntheses and in situ real-time atomic force microscopy of the $(ET)_2I_3$ and $Pe_2(ClO_4)$ overlayers were performed in a commercially available fluid cell (Digital Instruments, Santa Barbara, CA) adapted for electrochemical growth, as described previously.[13,14] A three-electrode design was employed for electrochemical measurements with a highly oriented pyrolytic graphite (HOPG) substrate (Union Carbide) serving as the working electrode, and Pt counter and reference electrodes placed in the outlet of the fluid cell. The HOPG substrate electrode was cleaved to expose a fresh surface prior to use. Overlayers of $(ET)_2I_3$ and $(Pe)_2ClO_4$ were grown by electrochemical oxidation of ET and Pe, respectively, in acetonitrile containing the respective electrolytes under conditions similar to those previously reported for the electrosynthesis of bulk crystals.[5(a),15,16] Au(111) substrates for deposition of the (TTF)(TCNQ) overlayers were prepared by melting high-purity gold wire (99.999%) in a oxygen/hydrogen flame to expose (111)-oriented facets.

Scanning tunneling (STM) and atomic force microscope (AFM) experiments were performed with a Nanoscope III Multimode scanning probe microscope (Digital Instruments, Santa Barbara, CA). STM tips consisted of mechanically cut Pt/Ir wires and AFM probes (Nanoprobe, Park Scientific, Sunnyvale, CA) consisted of triangular silicon nitride cantilevers (the force constant is $\approx 0.06\ N\ m^{-1}$) with integrated pyramidal tips. The AFM was equipped with a scan head having a maximum scan range of 12 by 12 μm^2, while the STM employed a scanner with a maximum range of 5 by 5 μm^2. AFM images were acquired in the contact mode under nominally constant force conditions, with integral and proportional gains of 4.0 and 7.0, respectively. The tip-sample force was minimized before imaging by reducing the set point to a value just below tip disengagement. The azimuthal orientations of the $(ET)_2I_3$ and $Pe_2(ClO_4)$ overlayers with respect to the HOPG substrate were determined by imaging an exposed region of the substrate immediately before or after imaging of the overlayer, or by imaging the substrate lattice underneath the overlayer after removing the overlayer mechanically by increasing the force exerted by the AFM tip.

Potential-energy calculations for the overlayer-substrate interfaces were performed on a Hewlett-Packard 710 workstation with a universal force field[17] based on a Lennard-Jones 6-12 potential function integrated with a customized Fortran code that allowed approach, translation, and rotation of a overlayer-substrate molecular interface. Energy-minimized overlayer structures and intralayer potentials were calculated using the Cerius molecular modeling program (Molecular Simulations, version 1.6) and the universal force field. Electrostatic interactions were neglected in these calculations, as it was determined that the results were rather insensitive to these contributions owing to their long-range nature. The native structures of the overlayers were surmised from layered motifs in bulk crystals whose structures were obtained from the Cambridge Structural Database (version 2.3.7). These native structures served as the initial trials in energy minimization and intralayer potential calculations. Stress and elastic constants were calculated directly from the calculated potentials. Structural models were visualized with the Computer-Assisted Chemistry (CAChe, Inc.) molecular modeling program. Calculations of interface misfit and epitaxy using the analytical function described here were performed on either the 710 workstation, or on an IBM 486 personal computer using a program written in our laboratory (EPICALC), which runs in the WINDOWS version 3.1 environment. EPICALC is available on the World Wide Web at http://www.cems.umn.edu/research/ward.

RESULTS AND DISCUSSION

The spatial configuration of a molecule or assembly of molecules at an interface is determined by a minimum in the total system energy. The potential energy of an atom B residing near a substrate plane of atoms A, assuming strict additivity of interaction energies between neighboring atoms, is the sum of interactions between atom B and the individual atoms in layer A.[18] If atom B belongs to a semi-infinite layer,

the total potential energy of the entire system, V_T, can be described by Eq. (1),

$$V_T=\sum_i \sum_j V_{AB}[(xy)_i^B-(xy)_j^A] + \tfrac{1}{2}\sum_{k\neq j} V_{AA}[(xy)_k^A-(xy)_j^A] + \tfrac{1}{2}\sum_{i\neq l} V_{BB}[(xy)_i^B-(xy)_l^B] \quad (1)$$

where $(xy)^A$ and $(xy)^B$ represent the positions of the atoms at some coordinate (xy) in layers A and B, respectively. The interaction energies between atoms in layers A and B are given by V_{AB}, while the last two terms represent the self-energies of the substrate and overlayer, respectively.

The optimum overlayer-substrate configuration can be determined by minimizing V_T with respect to the structure of the overlayer, and its separation, position, and azimuthal orientation with respect to the substrate. Such computations can be daunting due to the large number of possible overlayer-substrate configurations. Furthermore, the total system energy is not a strictly convex function, which makes determination of the global minimum configuration difficult and mathematically uncertain. This problem can be simplified by assuming the substrate structure is constant and unaffected by the overlayer, so that the term containing the substrate potential V_{AA} has a fixed value. This allows reduction of Eq. (1) to a form including only V_{AB} and V_{BB}. The relative magnitudes of the variations (δV) in these potentials with respect to changes in atomic coordinates will dictate whether the overlayer retains it native form $(\delta V_{BB}>\delta V_{AB})$ or is reconstructed $(\delta V_{AB}>\delta V_{BB})$. The total potential V_T will be decreased when epitaxy reinforces attractive interactions between the overlayer and substrate.

Epitaxial interface

Epitaxy generally is used to describe lattice registry, or, equivalently, the degree of ''phase matching,'' between two opposing lattice planes (although it was originally used to describe the growth of material B on substrate A, with B adopting the structure of A). In simple atomic systems, the criterion used to describe the extent of epitaxy along a specified crystallographic direction is the lattice misfit $f=(b-a)/a$, where a and b are lattice constants of the substrate and overlayer, respectively.[19] The misfit f is a one-dimensional parameter, and can be used for two-dimensional systems only when the two lattices are of equivalent symmetry and size. Therefore, an alternative approach is required for generic two-dimensional interfaces.

A two-dimensional interface consisting of substrate A and overlayer B can be described by seven parameters (Fig. 1). The substrate can be described by lattice constants a_1 and a_2 and angle α, the overlayer by b_1 and b_2 and angle β, and the azimuthal orientation can be defined by the angle θ between a_1 and b_1. The azimuthal relationship between substrate A and overlayer B can be described by a transformation matrix $\mathbf{C}$ which relates $\mathbf{b}_1$ and $\mathbf{b}_2$ to $\mathbf{a}_1$ and $\mathbf{a}_2$, where $\mathbf{C}$ is a 2×2 matrix with elements p_x, q_y, q_x, and p_y [Eq. (2)]. The values of the matrix elements depend upon the substrate lattice constants, the overlayer lattice constants, and θ according to Eqs. (3)–(6):

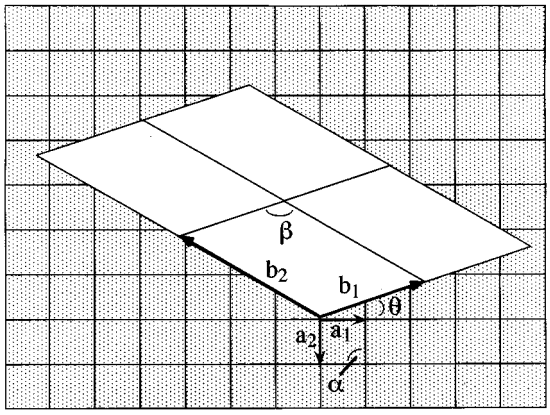

FIG. 1. Schematic representation of a generic 2×2 molecular overlayer on a rigid substrate. The substrate and overlayer lattices are defined by two-dimensional cells with lattice constants a_1, a_2, and α and b_1, b_2, and β, respectively. The angle θ represents the angle between the vectors $\mathbf{a}_1$ and $\mathbf{b}_1$, defining the azimuthal angle of the overlayer with respect to the substrate.

$$\begin{bmatrix} b_1 \\ b_2 \end{bmatrix} = [\mathbf{C}] \begin{bmatrix} a_1 \\ a_2 \end{bmatrix} = \begin{bmatrix} p_x & q_y \\ q_x & p_y \end{bmatrix} \begin{bmatrix} a_1 \\ a_2 \end{bmatrix}, \quad (2)$$

$$p_x = b_1 \sin(\alpha-\theta)/a_1 \sin(\alpha), \quad (3)$$

$$q_y = b_1 \sin(\theta)/a_2 \sin(\alpha), \quad (4)$$

$$q_x = b_2 \sin(\alpha-\theta-\beta)/a_1 \sin(\alpha), \quad (5)$$

$$p_y = b_2 \sin(\theta+\beta)/a_2 \sin(\alpha). \quad (6)$$

The primary value of the transformation matrix is that it describes the interface in convenient terms. This is particularly true for simple (atomic) lattices, for which the determinant of $\mathbf{C}$ can be used conveniently to deduce whether the system is commensurate, coincident, or incommensurate. However, det($\mathbf{C}$) does not provide insight into the energetics of the interface; nor is it very useful for evaluating the epitaxy of more complex, coincident molecular overlayers. Coincidence is not as well recognized as commensurism or incommensurism, but it is the main tenet of the following discussion. Therefore, the characteristics of these epitaxial conditions is reviewed here in the context of the properties of this matrix.

Commensurism

This condition exists when every overlayer lattice site resides on a particular set of substrate lattice sites. Under this condition, det($\mathbf{C}$) and each of the matrix elements assume integral values. Consequently, the overlayer unit cell can be described by a minimum integral number of substrate unit cells at some rotation angle.

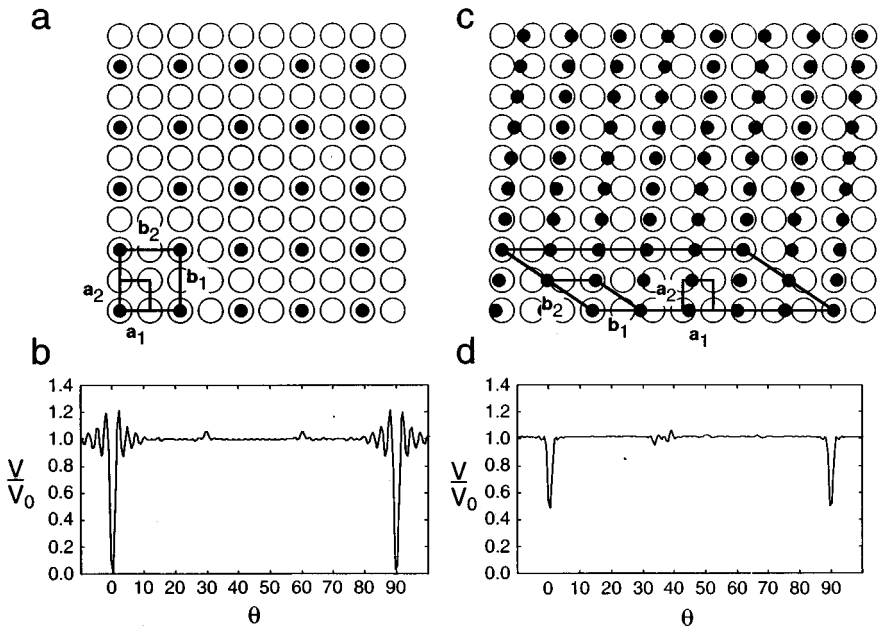

FIG. 2. (a) Schematic representation of a commensurate overlayer with $b_1=b_2=2a_1$ and $\beta=90°$ on a primitive substrate lattice with lattice constants $a_1=a_2$. (b) The dependence of the two-dimensional quasipotential V/V_0 on azimuthal angle θ for a 20×20 overlayer for the overlayer-substrate system in (a). The minimum at $\theta=0$ and 90° corresponds to the optimum epitaxy. (c) Schematic representation of a coincident overlayer with $b_1=1.6a_1$, $b_2=1.8a_2$, and $\beta=146.25°$. The 5×2 nonprimitive supercell, having vertices which are commensurate with the substrate, is depicted. (d) The dependence of the two-dimensional quasipotential V/V_0 on azimuthal angle θ for the overlayer-substrate system in (c). The minimum at $\theta=m\pi/2$ corresponds to the optimum epitaxy.

Coincidence

This condition exists when *rows* of overlayer sites are *coincident* with uniformly spaced *rows* of substrate sites corresponding to a specific lattice direction, such that one of the reciprocal-lattice vectors of the overlayer has the same direction as the reciprocal-lattice vector defined by the substrate rows (Fig. 2). The magnitude of the overlayer reciprocal-lattice vector is an integer multiple of the corresponding substrate lattice vector. There is commensurism with respect to these reciprocal-lattice vectors [$\mathbf{a}_1^*$ and $\mathbf{b}_1^*$ in Fig. 2(c)] while some overlayer sites are locally noncommensurate along the other lattice vectors [$\mathbf{a}_2$ and $\mathbf{b}_1$ in Fig. 2(c)]. The degree of epitaxy therefore is weaker than in a truly commensurate structure. Coincidence also implies the existence of a nonprimitive overlayer supercell, constructed from an integral number of overlayer unit cells, whose *perimeter* is commensurate with the substrate. This is equivalent to stating that some overlayer positions (most commonly chosen to be the vertices of the supercell) coincide with substrate sites at periodic intervals, while other positions contained within the supercell are locally noncommensurate. For a given system the degree of epitaxy, and therefore the energetics, will improve as the number of primitive overlayer cells necessary to construct the nonprimitive supercell decreases, as this leads to fewer non-commensurate overlayer sites.

det($\mathbf{C}$) for a coincident lattice will be a simple fraction. Coincidence further requires that certain combinations of the matrix coefficients assume integral values at the rotation angle θ. In the case of a generic lattice, p_x and q_x, or p_y and q_y, must be integers. Integral values for these combinations, or for the sums p_x+q_y and q_x+p_y, will produce coincidence on hexagonal substrates. Molecular overlayers will involve a large number of molecules assembled into two-dimensional lattices. The size and symmetry of these lattices will differ substantially from those of typical substrates, arguing against commensurate lattices in the absence of overlayer reconstruction. Consequently, any analysis of overlayer-substrate interfaces must consider the possibility of coincident overlayers.

Incommensurism

This condition exists when the overlayer is neither commensurate nor coincident with the substrate.

Two methods have been employed recently to evaluate epitaxy for molecular overlayers, specifically by examining the ''degree of epitaxy'' for continuously changing values of θ. The most complete method involves the determination of nonbonded potential-energy interactions summed over the entire overlayer-substrate interface. For a particular overlayer orientation and a fixed structure (in which the overlayer and substrate are considered to be rigid so that V_{AA} and V_{BB} are constant), the interface potential V_T can be described by Eq. (7),

$$V_T=\sum_i \sum_j V_{AB}(xy_i^B-xy_j^A), \tag{7}$$

which is a summation of the individual molecule-substrate potentials V_{AB}, where i and j refer to the summation over the substrate A and overlayer B atoms. The interaction potential V_{AB} can include van der Waals attraction, electron-

core repulsion, electrostatic interactions, and hydrogen bonding, which are generally weaker than covalent forces and are assumed to be pairwise additive such that the interaction between numerous atoms or molecules can be determined with a simple sum of individual atom-atom pair interactions using any one of several accepted empirical and semiempirical potential force fields.[20–23] It can be surmised from Eq. (7) that V_T will depend upon the azimuthal angle θ, with a global minimum in V_T at a value of θ at which epitaxy is maximized. However, for an overlayer and substrate, each having $n \times n$ atoms, the potential method requires n^4 calculations at each value of θ examined. This becomes prohibitive for computations involving large unit cells or large overlayers consisting of multiple unit cells. Furthermore, the semiempirical nature of these calculations does not guarantee accuracy.

An alternative method for determining the influence of periodic interfacial interactions at a two-dimensional interface has been reported in which the local misfits f between individual atomic or molecular sites in the overlayer and substrate are summed over the entire interface.[11] The summation can be described by the two-dimensional misfit parameter $D(\theta)$ in Eq. (8),

$$D(\theta)=\sum_i \sum_j \left| (ij)\{[\mathbf{C}]-\mathrm{int}[\mathbf{C}]\}-\begin{pmatrix} a_1 \\ a_2 \end{pmatrix} \right|, \tag{8}$$

where a_1 and a_2 represent the substrate lattice dimensions, and $\mathbf{C}$ is the transformation matrix defined above relating the overlayer and the substrate. This function simply sums the distances between overlayer and substrate lattice sites, in which the overlayer lattice sites are indexed to the nearest substrate lattice point by integers i and j. This is a discrete two-dimensional misfit calculation in which the energy units are arbitrary, and the value of θ at which $D(\theta)$ is minimum signifies the azimuthal angle at which epitaxy is maximized. If the system is coincident, one vector component of the misfit will disappear, and the depth of the minimum will depend upon the sum of misfit, reaching a maximum value for incommensurate overlayers. This method is conceptually simple, retains the essential features of the complete potential-energy calculation, and requires only n^2 calculations per configuration. However, it suffers from being a numerical method rather than an analytical one, has little direct theoretical significance, and remains computationally intensive if many overlayer cell structures and orientations are to be analyzed.

An analytical approach to epitaxy characterization

The computational intensiveness of these methods prompted us to develop an analytical method for evaluating epitaxy for overlayer-substrate systems. This method, which is based on an extension of earlier treatments for simple one- and two-dimensional lattices,[19,24,25] relies on a dimensionless potential energy V/V_0. For a one-dimensional lattice V/V_0 can be described by Eq. (9),

$$\frac{V(x)}{V_0}=\cos\left(\frac{2\pi}{a}x\right), \tag{9}$$

where a represents the lattice periodicity.

The interaction between a substrate lattice and an overlayer lattice is governed by the overlap of their potential-energy surfaces, with these interactions reinforced when the lattices are ''in phase.'' The potential of a one-dimensional *interface* is continuous, and can be described by Eq. (10),

$$\frac{V}{V_0}=\frac{\sum_i \left[1-\cos\left(\frac{2\pi b}{a}i\right)\right]}{\sum_i}, \tag{10}$$

where b is the overlayer unit-cell constant, and i has integral values of $i=0,\pm 1,\ldots,\pm m$. This can be expressed in terms of the mathematically equivalent Eq. (11),

$$\frac{V}{V_0}=\left[(2m+1)-\frac{\sin[(2m+1)\pi(f+1)]}{\sin[\pi(f+1)]}\right]\left(\frac{1}{2m+1}\right), \tag{11}$$

which is realized by replacing the summation with an integral, and defining the mismatch between the lattice periods a and b by the lattice misfit $f=(b-a)/a$. The V/V_0 term in Eq. (11) is a dimensionless potential whose value is governed by the ''degree of commensurability'' between the two one-dimensional lattices with respect to the misfit f. The term M is a whole number corresponding to multiples of lattice b, and $1/(2m+1)$ is a normalization constant. Under conditions where the lattice period b approaches the value of $a(f=0)$, the dimensionless potential tends to the minimum value of $V/V_0=0$ [evaluation of the sin terms in Eq. (11) at $f=0$ actually results in an indeterminant number of 0/0, but the theorem of de l'Hopital can be used to demonstrate that $V/V_0=0$ at $f=0$]. As f increases, V/V_0 actually increases through a maximum, before decreasing again in an oscillatory fashion. At large misfit, V/V_0 reaches a constant value of one. Equation (11) provides an analytical expression which can be used to establish the overlayer-substrate configuration at which V/V_0 is minimized, that is, at a configuration representing the best match between the two lattices.

This method can be extended to generic two-dimensional overlayer-substrate interfaces by adopting the previously reported approach, which only addressed trivial two-dimensional lattices. In this case, the dimensionless potential for an overlayer with unit-cell dimensions b_1 and b_2 can be described by Eq. (12),

$$\frac{V}{V_0}=\frac{\frac{1}{2}\sum_i\sum_j\left\{2-\cos\left[2\pi(ij)[\mathbf{C}]\begin{pmatrix}1\\0\end{pmatrix}\right]-\cos\left[2\pi(ij)[\mathbf{C}]\begin{pmatrix}0\\1\end{pmatrix}\right]\right\}}{\sum_i\sum_j}, \tag{12}$$

in which the lattice sites are indexed to substrate lattice sites by integers i and j. This expression incorporates the continuous nature of the interface potentials and also matrix **C**, which describes the azimuthal relationship between the overlayer and substrate. The overlayer sites along one of the Cartesian directions (x_i) are indexed to the substrate sites along this direction by the integer i, where i has integral values ranging from $-m$ to m, and their positions defined by the matrix **C**. Similarly, overlayer sites along the other Cartesian direction (y_j) are indexed to the substrate sites along this direction by the integer j, where j has integral values ranging from $-n$ to n. These relationships can be surmised readily from Eq. (2). The terms M and N correspond to the multiples of overlayer unit cell vectors b_1 and b_2 used in the calculations. The product $\mathbf{M}\times\mathbf{N}$ corresponds to the number of overlayer unit cells used in the calculation, where $M=2m+1$ and $N=2n+1$. This summation again can be replaced by an integral to give the analytical function in Eq. (13),

$$\frac{V}{V_0}=\left\{2(2m+1)(2n+1)-\frac{\sin[(2m+1)\pi p_x]\sin[(2n+1)\pi q_x]}{\sin[\pi p_x]\sin[\pi q_x]}-\frac{\sin[(2m+1)\pi q_y]\sin[(2n+1)\pi p_y]}{\sin[\pi q_y]\sin[\pi p_y]}\right\}\times\left(\frac{1}{2(2m+1)(2n+1)}\right), \tag{13}$$

in which $1/[2(2m+1)(2n+1)]$ is a normalization constant that ensures that V/V_0 has specific numerical values under certain conditions.

The potential V/V_0 can be calculated for azimuthal orientations defined by the component of matrix **C** for an overlayer with $M\times N$ unit cells. This potential varies continuously with orientation but adopts specific values for commensurism, coincidence, and incommensurism of 0, $\frac{1}{2}$, and 1, respectively. Notably, the computational requirements for determining misfit with Eq. (13) are minimal as a calculation at a particular value of θ requires only one operation, and is independent of overlayer size, in contrast to the aforementioned methods. The validity of this approach can be illustrated by comparing the azimuthal orientation of model systems with that predicted from of Eq. (13). For a substrate having lattice constants $a_1=a_2$ and a 20×20 overlayer of identical symmetry but with lattice constants of $b_1=b_2=2a_1$, V/V_0 passes through a minimum at $V/V_0=0$ at $\theta=0°$ and $\theta=90°$, as surmised by visual inspection of these lattices (Fig. 2). The value of $\det(\mathbf{C})=4$ for this commensurate overlayer is identical to the 4:1 ratio of unit-cell areas. As the azimuthal angle of the overlayer departs from the commensurate orientation, V/V_0 increases in an oscillatory manner due to the increasing misfit. Regions of incommensurism are signified by a value of $V/V_0=1$. The coincident condition can be illustrated by a substrate having lattice constants $a_1=a_2$ and an overlayer of different symmetry with lattice constants of $b_1=1.6a_1$, $b_2=1.8a_2$, and $\beta=146.25°$. Rows of overlayer lattice sites along $\mathbf{b}_1$ are coincident with substrate rows oriented along $\mathbf{a}_1$, and the reciprocal-lattice vectors $\mathbf{a}_1^*$ and $\mathbf{b}_1^*$ are identical. Calculation of V/V_0 predicts the presence of coincidence at $\theta=0°$ and 90°, as surmised by visual inspection of these lattices. This overlayer is described by a 5×2 nonprimitive supercell whose vertices are commensurate with the substrate.

The total potential V_T, two-dimensional misfit $D(\theta)$, and

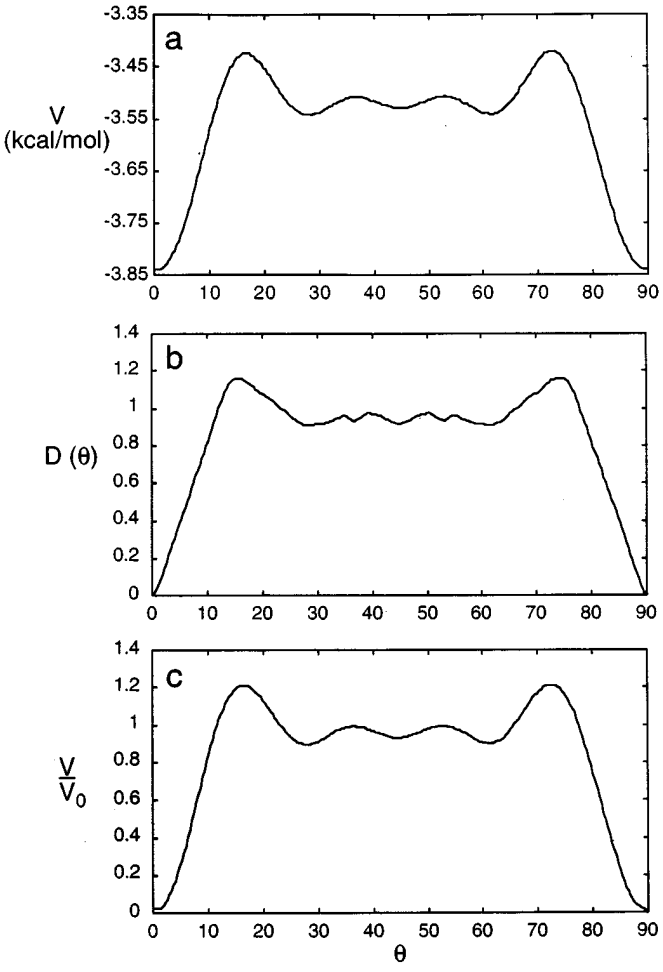

FIG. 3. Calculation of (a) V_T, (b) $D(\theta)$, and (c) V/V_0 for a 5×5 overlayer on a substrate with $a_1=a_2=b_1=b_2$. The total potential V_T was calculated with a Lennard-Jones 6-12 potential using Ar atoms as the basis.

V/V_0 for a trivial 5×5 overlayer and substrate, in which $a_1=a_2=b_1=b_2$ and $\alpha=\beta=90°$, each exhibit minima at orientations of $\theta=0°$ and $\theta=90°$ (Fig. 3) corresponding to a commensurate condition. The shape of $D(\theta)$ differs somewhat from the other two functions due to its discrete and linear nature. These data indicate that the dependence of V_T on θ is exactly reproduced with V/V_0 for this overlayer-substrate interface. Actual molecular overlayers are likely to exhibit differences in V_T and V/V_0, as V/V_0 does not account for local molecule-substrate interactions. However, as the overlayer size is increased, these local contributions will become increasingly dominated by the in-phase components so that only the periodic terms remain and the forms of V_T and V/V_0 converge to the same global minimum. This can be illustrated by examining an interface comprising a substrate with $a_1=a_2=2.46$ Å and $\alpha=60°$ (graphite) having two atoms per unit cell, and an overlayer with $b_1=6.61$ Å, $b_2=9.1$ Å, and $\beta=110°$ having three atoms (molecules) per unit cell [this particular overlayer corresponds to one that mimics the triiodide layer in the (001) plane of β-$(ET)_2I_3$, which is described below]. Differences in form and minima are evident for a 3×3 overlayer. However, the two functions progressively converge to the same form upon increasing overlayer size (5×5 and 7×7), eventually exhibiting identical minima at $\theta=19°$, where the value of $V/V_0=0.5$ indicates coincident epitaxy (Fig. 4). Therefore, V/V_0 is identical in form to the purely periodic components of V_T in the limit of increasingly larger overlayer sizes. *This illustrates that calculations performed with any of these methods must include a sufficient number of overlayer unit cells in order to establish accurately the phase relationship between the substrate and the overlayer.*

The validity of using V/V_0 to evaluate epitaxy can be demonstrated further by comparing the azimuthal angles observed experimentally for several overlayer-substrate systems to those calculated from V/V_0 using the known lattice parameters (Table I). In nearly every example in Table I, the orientation of the overlayer predicted by V/V_0 corresponds to that determined experimentally. Particularly interesting are the six polymorphs of perylene-tetracarboxylic dianhydride (PTCDA) overlayers, for which all but one are epitaxial by coincidence based on V/V_0. Figures 5 and 6 illustrate the V/V_0 dependences on θ for selected overlayer-substrate systems from Table I, and schematic representations of their corresponding orientations.[26–31] (Also see Fig. 7.)

These comparisons demonstrate that a simple dimensionless potential V/V_0 can be used to analyze and predict the registry of overlayer-substrate combinations, enabling a determination of the type of epitaxy and optimum azimuthal orientation for a particular overlayer structure. The computational time required for this analysis is independent of overlayer size, which is particularly important for analyzing molecular films with large, low-symmetry, oblique unit cells containing large numbers of basis atoms. The dependence of V_T and V/V_0 on overlayer size depicted in Fig. 4 illustrates that calculations performed on coincident overlayers, either with the total potential or V/V_0, can exhibit shallow and multiple potential minima if the overlayer sizes are small. The emergence of a clear global minimum associated with coincident overlayers for large overlayer sizes demonstrates that multiple minima or shallow potential functions observed

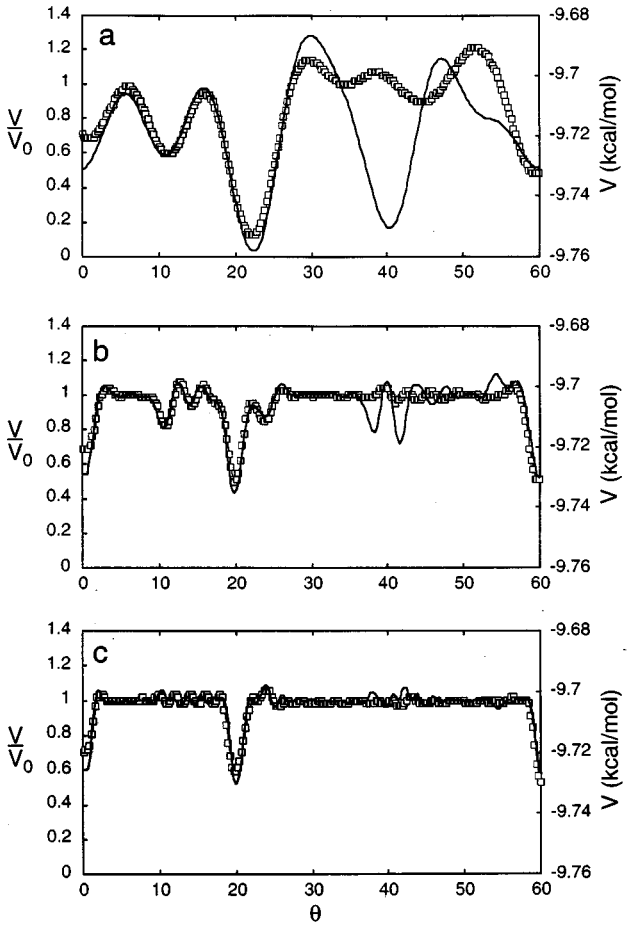

FIG. 4. Dependence of total interaction potential $V_T(\mathbf{r})$ and V/V_0(—) on overlayer size for an overlayer with $b_1=6.56$ Å, $b_2=9.1$ Å, $\beta=109.8°$, and a HOPG substrate with $a_1=2.46$ Å, $a_2=2.46$ Å, and $\alpha=120°$. Overlayer sizes: (a) 3×3, (b) 5×5, and (c) 7×7. In the calculation of V_T, the substrate is graphite, which contains two atoms per unit cell, the overlayer is the I_3^- layer of the (001) plane of β-$(ET)_2I_3$, which contains three I atoms per unit cell.

for small overlayer sizes does not necessarily signify incommensurism. The concept of ''quasiepitaxy,'' a condition surmised from an apparent lack of commensurism, was advanced recently to explain the formation of low-defect molecular overlayers.[8] However, evaluation of V/V_0 for several overlayers (Table I) reveals that most of these are actually *coincident*, with clearly defined minima at the azimuthal angles indicated. The existence of coincidence does not detract from the ability to form stress-free, low-defect molecular overlayers. Indeed, the ability of overlayers to be stabilized by coincidence in their essentially unreconstructed state is an ideal condition for the formation of high-quality crystalline multilayers and bulk materials grown from these primary overlayers.

The computational efficiency of this analytical function also enables systematic searching, within a reasonable time, for reconstructed overlayers whose lattice parameters b_1, b_2, and β are bracketed around the native overlayer values, so that possible epitaxy-driven reconstructions can be examined. This is performed with a custom-made program, developed in our laboratory, operating in the WINDOWS environment, which calculates V/V_0 over the full range of θ for

TABLE I. Comparison of the experimentally measured and calculated azimuthal angles (θ_{expt} and θ_{calc}, respectively) for various overlayer-substrate systems with overlayer lattice constants b_1, b_2, and β.

Organic overlayer	Substrate[a]	b_1 (Å)	b_2 (Å)	β (deg)	θ_{expt} (deg)	θ_{calc} (deg)	Supercell size[b] $M\times N$	Method	Ref.
PTCDA	MoS_2[c]	12.4	19.7	88.8	12.7	12.7	3×1	STM	26
	HOPG[c]	15.2	21.6	90.0	13	±11.3	3×3	STM	8(a), 8(b), 27
	HOPG[c]	15.7	20.0	90.0	19	±18.6	3×2	Theor	8(a), 8(b), 27
	HOPG[c]	12.7	19.2	89.5	3.1	3.2	3×1	STM	11
	HOPG[c]	12.4	19.4	90.0	9.9	±9.9	2×1	STM	11
	HOPG[c]	12.0	20.2	90.0	2.5	±2.3	3×3	LEED	6(c), 6(c)
	HOPG[c]	12.5	19.1	90.0	3.0	[d]		LEED	6(b), 6(c)
	HOPG[c]	12.7	19.2	89.5	3.2	3.2	3×1	STM	6(b), 6(c)
	Cu(100)[e]	14.5	18.1	90.0	45	45	1×1	LEED	28
PTCDI	HOPG[c]	14.5	16.9	83.6	12.7	12.7	2×2	STM	6(b), 6(c)
	MoS_2[c]	14.5	17.2	83.1	10.9	10.8	1×3	STM	6(b), 6(c)
CuPc	MoS_2[e]	13.7	14.2	90.0	30	30	2×2	STM	29
	Cu(100)[e]	13.8	19.0	96.6	23.4	22.2	1×1	LEED	28
	Cu(111)[c]	12.6	12.6	85.0	8	0,35	1×3	LEED	30
FePc	Cu(100)[e]	13.7	13.7	90.0	22.5	±21.8	1×1	LEED	30
	Cu(111)[c]	12.0	12.0	82.0	11	[b]		LEED	30
Pc	Cu(100)[e]	13.7	13.7	90.0	22.5	±21.8	1×1	LEED	30
	Cu(111)[c]	13.3	13.3	81.5	10.25	±11	3×1	LEED	30
$(Pe)_2ClO_4$	HOPG[c]	10.9	18.1	87.0	15	9	5×2	AFM	5(b)
(TTF)(TCNQ)	Au(111)[c]	11.0	16.5	104.0	[f]	27	5×4	STM	31
β-$(ET)_2I_3$-I[g]	HOPG[c]	6.6	9.1	110.0	18	19	1×3	AFM	5(a)
β-$(ET)_2I_3$-II	HOPG[c]	7.2	17.3	83.0	15	17	3×5	AFM	5(b)

[a]Lattice constants for substrates: HOPG ($a_1=a_2=2.46$ Å/$\alpha=60°$), MoS_2 ($a_1=a_2=3.16$ Å/$\alpha=60°$), Cu(100) ($a_1=a_2=3.61$ Å/$\alpha=90°$); Cu(111) ($a_1=a_2=2.56$ Å/$\alpha=60°$); Au(111) ($a_1=a_2=2.88$ Å/$\alpha=60°$).

[b]M and N refer to the multiples of b_1 and b_2 describing the overlayer supercell. In cases where the supercell did not fit the substrate perfectly, the supercell dimensions given represent values corresponding to <5% misfit along one overlayers lattice vector.

[c]Coincident.

[d]Incommensurate.

[e]Commensurate.

[f]θ_{expt} was not determined due to experimental difficulties.

[g]Lattice parameters given correspond to those of the (001) plane of bulk β-$(ET)_2I_3$, which are identical to the lattice constants of the overlayer observed by AFM, within experimental error bulk crystal.

numerous sets of lattice parameters. Computations performed on a standard 486 processor enable >1000 possible reconstructed forms to be searched and fully analyzed in 1 h. However, V/V_0 does not provide the actual overlayer-substrate interaction energy or stability ranking of different epitaxial overlayer-substrate combinations. Rather, its utility lies in narrowing the choice of possible configurations available to a particular overlayer-substrate system.

Energetics of the overlayer-substrate interface

Although epitaxy plays an important role in determining the orientation and stability of the overlayer-substrate interface, the actual *energetics* of the interface cannot be overlooked. The competition between intralayer and interlayer interactions can be described in terms of the elasticities of the overlayer and the overlayer-substrate interface, which are related to the corresponding interaction potentials.[8] Reconstruction of an overlayer accompanying the formation of commensurate or coincident lattices is tantamount to introducing intralayer strain, described by the difference between the positions of the molecules in the reconstructed and native forms. This strain will impart an intralayer stress that, for a sufficiently small strain, can be described by a linear stress-strain relationship. The stress and strain in a three-dimensional solid are second-rank tensors, and can be used to analyze the elastic properties of a thin-film–substrate interface (Fig. 8). Stresses between the overlayer and substrate due to molecules located on noncommensurate positions (σ_x^{inter}, σ_y^{inter}, and σ_z^{inter}) create interfacial forces which drive reconstruction of the overlayer toward commensurate forms. These stresses are opposed by intralayer stresses (σ_x^{intra} and σ_y^{intra}) accompanying reconstruction of the native overlayer structure. If only the purely extensional components of the strain tensor, parallel to the film interface and directed along x and y (ε_x and ε_y), are considered the stress-strain relations for the intralayer components are given by Eqs. (14) and (15),

$$\sigma_x^{intra}=c_{xx}^{intra}\varepsilon_x, \tag{14}$$

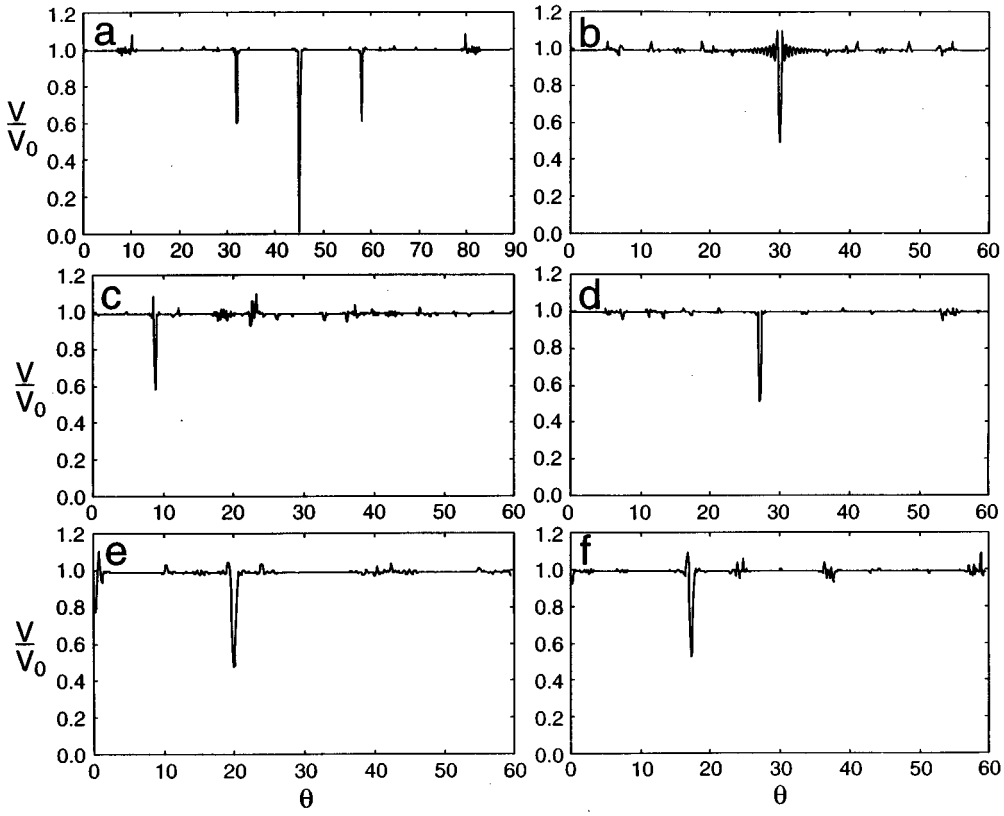

FIG. 5. Calculated dependence of V/V_0 on azimuthal angle θ for the selected overlayer-substrate combinations depicted in Fig. 6. (a) PTCDA‖Cu(100), (b) CuPc‖MoS_2, (c) $(Pe)_2ClO_4$‖HOPG, (d) (TTF)(TCNQ)‖Au(111), (e) β-$(ET)_2I_3$ (type I)‖HOPG, and (f) β-$(ET)_2I_3$ (type II)‖HOPG. The calculations were performed using 20×20 overlayers.

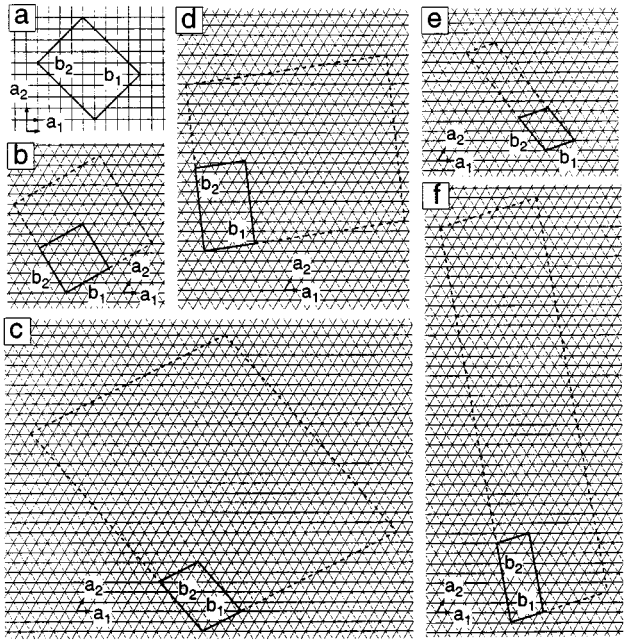

FIG. 6. Schematic representations of overlayer orientations on substrates for selected systems in Table I as viewed normal to the overlayer-substrate interface. The perimeter of the primitive overlayer unit cell is depicted by a solid line. The perimeter of the nonprimitive commensurate supercell for the coincident overlayers is depicted by the dashed line. (a) PTCDA‖Cu(100), (b) CuPc‖MoS_2, (c) $(Pe)_2ClO_4$‖HOPG, (d) (TTF)(TCNQ)‖Au(111), (e) β-$(ET)_2I_3$ (type I)‖HOPG, and (f) β-$(ET)_2I_3$ (type II)‖HOPG.

$$\sigma_y^{\text{intra}} = c_{yy}^{\text{intra}} \varepsilon_y . \tag{15}$$

The intralayer elastic constants c_{xx}^{intra} and c_{yy}^{intra} represent the ''stiffness'' of the overlayer, that is, its resistance to reconstruction from its preferred or native structure. The elastic constants can be determined by a calculation of the second derivative of the corresponding potential functions, the second derivative simply being the radius of curvature of the potential well, $\kappa = d^2V/dr^2$. The larger the value of κ, the larger the stiffness constant, and the greater the opposition to perturbations from the minimum-energy configuration. The radius of curvature of the potential generally will scale with its depth, implying that larger interaction energies generally will lead to larger elastic constants.

The stress component oriented normal to the substrate interface σ_z is related to the strain ϵ_z, which describes changes in the overlayer-substrate separation along the z axis, by the elastic constant c_{zz}^{inter} [Eq. (16)]. Strain at the overlayer-substrate interface along the x axis, such as that resulting from molecules sitting on locally noncommensurate positions in coincident overlayers, will result in a stress along x and a shear stress along z according to Eqs. (17) and (18),

$$\sigma_z^{\text{inter}} = c_{zz}^{\text{inter}} \epsilon_z , \tag{16}$$

$$\sigma_x^{\text{inter}} = c_{xx}^{\text{inter}} \epsilon_x , \tag{17}$$

$$\sigma_z^{\text{inter}} = c_{xz}^{\text{inter}} \epsilon_x . \tag{18}$$

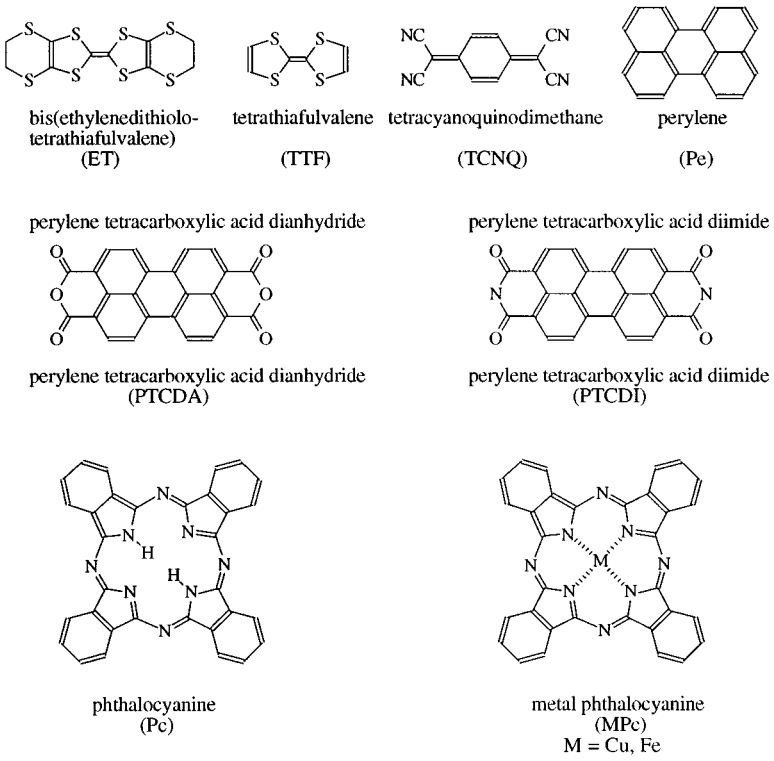

FIG. 7. Component of epitaxially grown molecular films described in Table I.

Small overlayer-substrate elastic constants and larger intralayer elastic constants will conspire to favor coincident overlayers, as the *interfacial* stress associated with molecules on nonideal positions will be smaller than the *Intralayer* stress that would accompany reconstruction of the overlayer from its native form to a reconstructed overlayer that is commensurate with the substrate. In contrast, large overlayer-substrate and small intralayer elastic constants will favor the formation of a strained (i.e., reconstructed from a native form) commensurate overlayer. The competition between interfacial and intralayer interactions and stiffness is evident from comparison of the PTCDA/Cu(100), PTCDA/HOPG, and PTCDA/MoS_2 systems. A highly reconstructed commensurate overlayer is observed on Cu(100), while on HOPG and MoS_2 coincident overlayers are observed with a structure comparable to those in the bulk crystal. The formation of a commensurate structure on Cu(100) suggests strong chemisorption on the high-energy Cu(100) surface. In contrast, the interfacial interactions, and the corresponding interfacial stresses, are expected to be smaller on the lower energy HOPG and MoS_2 surfaces, enabling the formation of coincident lattices for which intralayer forces dominate the overlayer structure.

Recent studies in our laboratory have demonstrated that molecular overlayers with structures mimicking layers in bulk crystals of conducting charge-transfer salts can be grown epitaxially on ordered substrates such as HOPG. Among the systems we investigated, three are illustrative of the influence of overlayer-substrate energetics: $(ET)_2I_3$‖HOPG, $(Pe)_2ClO_4$‖HOPG, and (TTF)(TCNQ)‖Au(111) (Fig. 9). The azimuthal orientations of the overlayers for $(ET)_2I_3$‖HOPG and $(Pe)_2ClO_4$‖HOPG were established directly by atomic force microscopy during electrochemical growth of these monolayers in solution.[5(a),5(b)] This was accomplished by obtaining lattice images of the overlayer, and comparing their orientation to the bare substrate lattice in regions either adjacent to the overlayer or beneath the overlayer (produced after mechanical etching of the overlayer with the AFM tip). The overlayer structures, all of which were coincident with the HOPG substrate, reflect the balance between interfacial and intralayer elasticity (Table II). In the case of $(ET)_2I_3$, a coincident overlayer was observed whose lattice constants were identical, within experimental error, to those of the molecular (001) layers in the bulk crystal of β-$(ET)_2I_3$. Analysis of V/V_0 based on the bulk crystal lattice parameters for β-$(ET)_2I_3$ for this overlayer indicated coincidence at $\theta=19°$, in near agreement with the experimentally observed value of $\theta=18°$.

This coincident β-$(ET)_2I_3$ overlayer is described by a 1×3 nonprimitive commensurate supercell which contains molecules within its perimeter that reside on noncommensurate lattice positions. The nonideality of these positions represent local strains, but calculations indicate that the interfacial stresses resulting from these strains are likely to be small. The calculated adsorption energy for a (001) β-$(ET)_2I_3$ unit cell on HOPG was 15.1 kcal mol^{-1} (at $\theta=0°$), and the dependence of potential V on translation and azimuthal rotation was rather shallow, varying only by 0.2 kcal mol^{-1}. This is tantamount to small interfacial elastic constants c_{xx} and c_{xz}, and, consequently, the stresses σ_z and σ_x associated with placing molecules on noncommensurate position are rather small [Figs. 8(c) and 8(d)]. In contrast, the potential-well depths, and accordingly the stress and elastic constants, associated with the *intralayer* interactions are significantly larger than the interfacial values (Table I). This signals that the energetic penalty resulting from reconstruction of the coincident overlayer to a commensurate overlayer is greater than the energetic penalty associated with the noncommensurate overlayer sites in the coincident structure. The observations of an unreconstructed β-$(ET)_2I_3$ (001) overlayer can

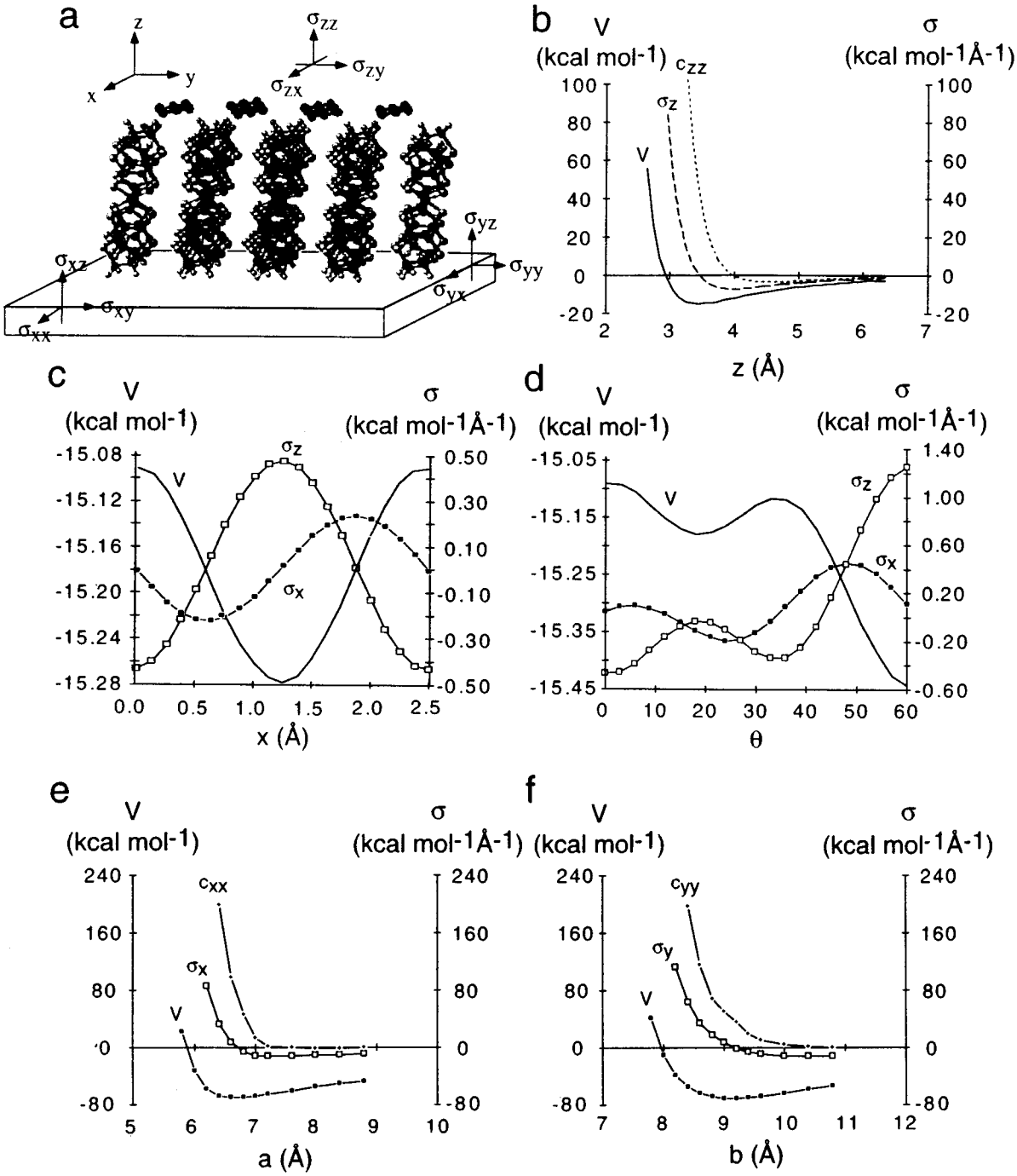

FIG. 8. (a) Schematic representation of the overlayer-substrate interface for the β-$(ET)_2I_3$ (type I)‖HOPG in which the structure of the overlayer mimics that of the (001) molecular layers present in β-$(ET)_2I_3$. The stress components σ_{xx} and σ_{yy} represent purely intralayer stress resulting from extensional strain in the overlayer, σ_{xy} and σ_{yx} represents intralayer shear stress resulting from extensional strain, σ_{zz} represents the interfacial stress due to changes in the overlayer-substrate separation, and σ_{xz}, σ_{yz}, σ_{zx} and σ_{zx} are shear stress components. (b) The dependence of the total interaction potential (V_T), stress ($\sigma_z = dV_T/dz$), and elastic constant ($c_{zz} = d^2V_T/dz^2$) upon overlayer-substrate separation z for (001) β-$(ET)_2I_3$‖HOPG for a 1×1 overlayer. (c) Changes of V_T, σ_x, and σ_z upon translation of a 1×1 (001) β-$(ET)_2I_3$ overlayer on the HOPG surface along $\mathbf{a}_1$. The overlayer-substrate separation was fixed at 3.4 Å. (d) Changes of V_T, σ_x, and σ_z upon rotation of the (001) β-$(ET)_2I_3$ overlayer on the HOPG surface about a fixed axis perpendicular to the interface. The overlayer-substrate separation was fixed at 3.4 Å, and the origin of the (001) β-$(ET)_2I_3$ unit cell was fixed at the mimimum established in (b). The local minimum at $\theta = 19°$ reflects the minimum observed for large overlayer sizes (see Fig. 4), whereas the deeper minimum evident at 60° is a false minimum resulting from the small overlayer size used in the calculation. (e) and (f) Dependence of V, σ_x, σ_y, c_{xx}, and c_{yy} for an isolated the (001) β-$(ET)_2I_3$ layer. The minima of the potential wells are $a = 6.67$ and 9.09 Å, essentially identical to the corresponding values of $a = 6.61$ Å and $b = 9.1$ Å observed for the (001) layer in the bulk crystal. Interaction potentials were determined using a universal force field.

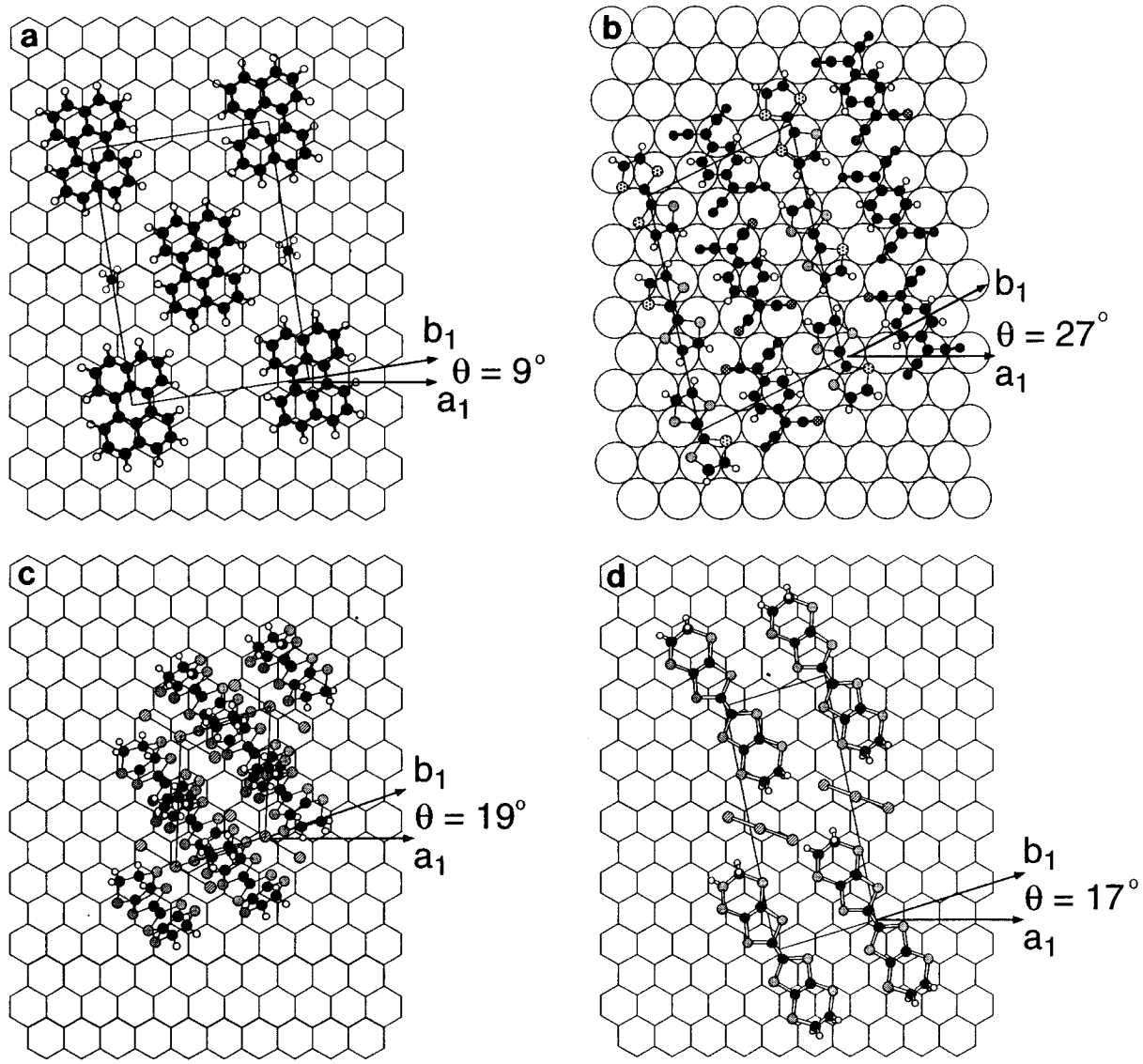

FIG. 9. Schematic illustration of overlayers on substrates for (a) $(Pe)_2ClO_4$ on HOPG, (b) (TTF)(TCNQ) on Au(111), (c) β-$(ET)_2I_3$ type I on HOPG, and (d) β-$(ET)_2I_3$ type II on HOPG. The overlayer structures are depicted with lattice constants and azimuthal orientations (θ) corresponding to those observed experimentally, which agree with the values calculated from V/V_0. The actual orientation of the molecules in the overlayers are not known rigorously, and their orientations here are based on their orientations in the corresponding bulk crystals.

be attributed to strong intralayer interactions and large elastic constants associated with strong π-π interactions along the ET stacks and in-plane S-S interactions between ET molecules in a direction perpendicular to these stacks, but weak van der Waals interactions between (001) layers which serve to minimize the surface energy of this plane. Indeed, the energy-minimized structure of the (001) layers was essentially identical to that observed in the bulk crystal. The ability of this native form to achieve coincidence provides sufficient stabilization of the overlayer, so that energetically unfavorable reconstruction to a commensurate overlayer is obviated. It is worth noting that analysis of V/V_0 for $(ET)_2I_3$ molecular layers in the numerous polymorphs or compositional variants of bulk crystals[32] did not reveal any coincident relationships with HOPG. These polymorphs contain layer structures, also with large intralayer elasticities, suggesting that the energetic penalty associated with reconstruction to coincident or commensurate structures is too large for these to be formed.

In contrast to the (001) β-$(ET)_2I_3$ overlayer, analysis of V/V_0 for molecular $(Pe)_2ClO_4$ (Ref. 33) and (TTF)(TCNQ) (Ref. 34) layers did not identify any native layers which were epitaxial with HOPG and Au(111) substrates, respectively.[35] Nevertheless, the AFM and STM revealed the formation of molecularly thick overlayers (~4 A) with lattice constants differing from those of the bulk layers or energy-minimized forms of these layers. Analysis of V/V_0 based on the AFM and STM lattice constants indicated that these overlayers were coincident at azimuthal angles of θ=9° and 27° for $(Pe)_2ClO_4$‖HOPG and (TTF)(TCNQ)‖Au(111), respectively. In the case of $(Pe)_2ClO_4$‖HOPG the calculated azimuthal angle was identical, within experimental error, to that measured by the AFM. Experimental difficulties related to the stability of the (TTF)(TCNQ) overlayers on Au(111) during scanning with the STM have thus far prevented reliable determination of the azimuthal angle for this system. However, we presume that it is coincidence at θ=27° that stabilizes this overlayer. The 4-Å thickness of the overlayers in each

TABLE II. The azimuthal angle, lattice constants, adsorption energies, and variation of adsorption energies with respect to overlayer position, for molecular films based on charge-transfer salts. The experimental values of θ, $\mathbf{b}_1$, $\mathbf{b}_2$, and β were determined by either AFM or STM.

Overlayer	b_1 (Å)	b_2 (Å)	β (deg)	θ (deg)	c_{xx} intra (kcal mol^{-1} Å^{-2})	c_{yy} intra (kcal mol^{-1} Å^{-2})	c_{zz} inter (kcal mol^{-1} Å^{-2})	c_{xx} inter (kcal mol^{-1} Å^{-2})	c_{xz} inter (kcal mol^{-1} Å^{-2})
$(Pe)_2ClO_4$/HOPG									
Calculated	13.2	19.2	90	9[a]	6.6	5.4	167	1.74	3.51
AFM	10.9±0.6	18.1±0.8	87	15					
Bulk crystal (001 layer)[b]	13.1	14.1	90	[c]					
(TTF)(TCNQ)/Au(111)									
Calculated	12.7	18.4	104	[d]	13.5	6.5	27.9	0.71	1.71
STM	11.0±0.3	16.5±0.4	104	27[e]					
Bulk crystal (010) layer[f]	12.3	18.5	104	[c]					
(001) β-$(ET)_2I_3$/HOPG									
Calculated	6.67	9.09	110	19[a]	80.2	36	43.5	0.61	1.17
AFM	6.3±0.4	8.5±0.4	108	18[g]					
Bulk crystal (001 layer)	6.61	9.1	110	19					
(011) β-$(ET)_2I_3$/HOPG									
Calculated[a]	6.65	18.6	83	17[a]	36	5	192	2.96	6.49
AFM	7.2±0.4	17.3±0.8	83	15					
Bulk crystal (011) layer	6.67	18.4	82	[c]					

[a]The values of θ were calculated from from analysis of V/V_0 using the lattice constants b_1, b_2, and β calculated for the energy-minimized overlayer structure (entries to the right of this θ value) using the universal force field.

[b]The bulk lattice constants actually are those reported for $(Pe)_2PF_6$ (Ref. 34), but these are believed to be similar to those of the corresponding perchlorate salt.

[c]No epitaxial orientation was evident from analysis of V/V_0 based on the lattice constants of the crystal plane indicated in the entry to the left, or for any other reasonable crystal plane of the bulk crystal.

[d]No epitaxial orientation was evident from analysis grown from analysis of V/V_0 based on these calculated lattice constants of the reconstructed (010) crystal plane.

[e]The value of θ=27° was calculated based on the STM lattice constants. The actual azimuthal orientation could not be determined due to experimental limitations.

[f]Bulk crystal structure reported in Ref. 33.

[g]AFM measurements indicated θ values ranging from 10–19°, which is attributed to orientational disorder and small contributions from experimental error. However, a more reliable determination of θ was achieved by AFM performed microcrystals on the HOPG substrate grown from the overlayer, which indicated that θ=18°.

case suggested that the molecular planes were parallel to the substrates, resembling the (100) plane in $(Pe)_2ClO_4$ and the (010) plane in (TTF)(TCNQ). However, these overlayers are substantially reconstructed from their ''native'' forms, given the difference between the crystallographic constants and those determined by the AFM and STM (Fig. 8). Furthermore, the lattice constants of the energy-minimized layer structures also differed substantially from their native bulk forms. The intralayer interactions are primarily van der Waals in nature, with additional contributions from ion-ion interactions (the latter were disregarded in our calculations because parallel studies have indicated that their contribution was minimal due to their long-range nature). The calculated values given in Table II indicate that the intralayer elastic constants of the $(Pe)_2ClO_4$ overlayer are substantially smaller than those of the (001) β-$(ET)_2I_3$ overlayer, consistent with weaker intralayer interactions and reduced overlayer stiffness. Conversely, the calculated adsorption energy of a unit cell of $(Pe)_2ClO_4$ on HOPG is -92.4 kcal mol^{-1} (at θ=0°), and the variation in this energy is 0.8 kcal mol^{-1}, both substantially higher than that calculated for the (001) β-$(ET)_2I_3$ overlayer. This is due to stronger interfacial interactions associated with the Pe molecular planes lying parallel to the HOPG surface, which results in a greater dispersive interaction per molecule. Consequently, the interfacial elastics constants are substantially higher, and the energetic benefit of coincident epitaxy outweighs the penalty associated with the reconstruction required to achieve coincidence. However, the absence of a completely commensurate overlayer structure indicates that a severe reconstruction is energetically prohibitive. Similar arguments support the observation of a (TTF)(TCNQ) layer which is substantially reconstructed from its native (010) layer structure. We surmise that strong gold-sulfur interactions play an important role in the observed orientation and in the reconstruction of a lattice which is compressed compared to the bulk layer structure.

The delicate balance of these factors can be illustrated further by our observation of a second orientation of $(ET)_2I_3$ on HOPG, for which the overlayer structure resembles a reconstructed (011) layer from β-$(ET)_2I_3$ [recent experiments suggest that this layer may actually be the precursor of the (001) orientation]. This coincident overlayer is described by flat-lying molecules in which intralayer S-S heteroatom interactions are present but the π-π overlap is absent, which results in smaller intralayer interactions and elastic constants compared to the (001) orientation. The calculated absorption energy for this orientation was -40 kcal mol^{-1} (at $\theta=0°$) and the spread of adsorption energies was 0.8 kcal mol^{-1}, leading to larger interfacial elastic constants than those observed for the (001) orientation. These factors favor reconstruction of the native layer structure to a form that is coincident, but not commensurate.

These observations reveal the factors controlling the mode of overlayer growth. The most favorable growth mode will be that in which coincidence is achieved by an unreconstructed (or very slightly reconstructed) molecular layer with strong intralayer interactions. In this configuration the overlayer structure is at or near its energy minimum, the surface energy is minimized because the strongest interactions are within the plane of the overlayer, the intralayer stiffness exceeds that of the overlayer-substrate interface, and epitaxial stabilization can achieved by coincidence. If epitaxy with such an overlayer is not possible, its large intralayer elastic constant will inhibit the reconstruction required to achieve coincidence or commensurism. Under this condition the system will likely favor the growth of epitaxial overlayers whose structures resemble alternative bulk crystal planes with smaller intralayer interactions and elastic constants. This reduces the energetic penalty of overlayer reconstruction necessary to achieve epitaxy by either coincidence or commensurism. However, this can lead to growth orientations in which the strongest intermolecular interactions are perpendicular to the overlayer, as is the case for $(Pe)_2ClO_4$‖HOPG, $(011)\beta$-$(ET)_2I_3$‖HOPG, and (TTF)(TCNQ)‖Au(111). Under this condition, the elastic constants defining the interface between layers are expected to be large. Because the structure of a reconstructed primary overlayer differs from its bulk native form, this can lead to significant stresses during growth of multilayer thin films from these primary overlayers.

CONCLUSIONS

We have demonstrated that a simple analytical function can be used to analyze the epitaxy between molecular overlayers and rigid ordered substrates. This method predicts whether an overlayer is commensurate or coincident, and predicts the azimuthal angles required for these conditions. Comparison with total potential-energy calculations reveals that the dependence of overlayer-substrate potential upon azimuthal angle is reproduced by V/V_0. The validity of the analytical method is corroborated further by the good agreement of V/V_0 minima with the azimuthal orientations for numerous overlayer structures observed experimentally. The advantage of this approach is that the computation is independent of overlayer size, which enables rapid analysis for large basis sets and large overlayers. This is crucial for identifying coincident lattices as potential-energy calculations, which are necessarily limited to small numbers of overlayer unit cells due to their computational intensiveness, can yield shallow minima that incorrectly suggest incommensurism. The type of epitaxy and optimum azimuthal angle can be determined in seconds on a low-cost CPU, enabling convenient searching for possible reconstructed overlayer configurations in which the lattice parameters a_1, b_2, and β are bracketed around the native overlayer values so that slight epitaxy-driven reconstructions can be surmised. This method can be used to determine the likelihood of epitaxy of different polymorphic forms of an overlayer if these polymorph structures are known, providing some predictability of the overlayer structure. If these overlayers serve as nuclei for multilayers or bulk crystals, this can serve as a convenient approach to selecting substrates for selective crystallization of thin-film structures or crystals that tend to exhibit polymorphism. When combined with analysis of the elastic constants for a given overlayer-substrate configuration, this provides a convenient approach for the *a priori* design of heteroepitaxial molecular films and substrates for the growth of multilayer films and bulk crystals.

ACKNOWLEDGMENTS

The authors gratefully acknowledge Christopher M. Yip for writing the WINDOWS version of EPICALC. Financial support was provided by the Office of Naval Research and the Center for Interfacial Engineering, a National Science Foundation Engineering Research Center.

*Current address: Department of Chemical Engineering, University of Virginia, Charlottesville, VA 22902.

†Author to whom correspondence should be addressed.

[1] A. Aviram and M. Ratner, Chem. Phys. Lett. **29**, 277 (1974); *Molecular Electronic Devices*, edited by F. Carter (Marcel Dekker, New York, 1982); *Molecular Electronics*, edited by G. Ashwell (Wiley, New York, 1992).

[2] M. Matsumoto, T. Nakamura, E. Manda, and Y. Kawabata, Thin Solid Films **160**, 61 (1988); K. Naito, A. Miura, and M. Azuma, J. Am. Chem. Soc. **113**, 6386 (1991); A. Dhindsa, Y.-P. Song, J. Badyal, M. Bryce, Y. Lvov, and M. Petty, J. Chem. Mater. **4**, 724 (1992); C. M. Yip and M. D. Ward, Langmuir **10**, 549 (1994).

[3] G. Cao, H.-G. Hong, and T. E. Mallouk, Acc. Chem. Res. **25**, 420 (1992); M. E. Thompson, Chem. Mater. **6**, 1168 (1994).

[4] S. Yitzchaik, S. B. Roscoe, A. K. Kakkar, D. S. Allan, T. J. Marks, Z. Xu, T. Zhang, W. Lin, and G. K. Wong, J. Phys. Chem. **97**, 6958 (1993).

[5] (a) A. C. Hillier, J. B. Maxson, and M. D. Ward, Chem. Mater. **6**, 2222 (1994); (b) A. C. Hillier, Ph.D. thesis, University of Minnesota, 1995 (unpublished).

[6] (a) G. E. Collins, K. W. Nebesny, C. England, L. Chau, P. A. Lee, B. Parkinson, Q. Fernando, and N. R. Armstrong, J. Vac. Sci. Technol. A **10**, 2909 (1992); (b) C. Ludwig, B. Gompf, W. Flatz, J. Peterson, W. Eisenmenger, M. Mobus, U. Zimmermann, and N. Karl, Z. Phys. B **86**, 397 (1992); (c) C. Ludwig, B. Gompf, J. Peterson, R. Strohmaier, and W. Eisenmenger, *ibid*. **93**, 365 (1993); (d) N. R. Armstrong, K. W. Nebesny, G. E. Collins, L.-K. Chau, P. A. Lee, C. D. England, D. Diehl, M. Douskey, and B. Parkinson, Thin Solid Films **216**, 90 (1992); (e)

K. W. Nebesny, G. E. Collins, P. A. Lee, L.-K. Chau, J. Danziger, E. Osburn, and N. R. Armstrong, Chem. Mater. **3**, 829 (1991).

[7] *Epitaxial Growth*, edited by J. Matthews (Academic, New York, 1975).

[8] (a) S. R. Forrest and Y. Zhang, Phys. Rev. B **49**, 11 297 (1994); (b) Y. Zhang and S. R. Forrest, Phys. Rev. Lett. **71**, 2765 (1993).

[9] R. P. Scaringe, in *Electron Crystallography of Organic Molecules*, edited by J. R. Fryer and D. L. Dorset (Kluwer, Boston, 1991), p. 85.

[10] J. Perlstein, J. Am. Chem. Soc. **116**, 11 420 (1994).

[11] A. Hoshino, S. Isoda, H. Kurata, and T. Kobayashi, J. Appl. Phys. **76**, 4113 (1994).

[12] K. Bender, I. Hennig, D. Schweitzer, K. Dietz, H. Endres, and H. Keller, Mol. Cryst. Liq. Cryst. **108**, 359 (1984); T. J. Emge, P. Leung, and M. Beno, *ibid*. **132**, 363 (1986).

[13] A. C. Hillier and M. D. Ward, Science **268**, 1261 (1994).

[14] A. C. Hillier, P. W. Carter, and M. D. Ward, J. Am. Chem. Soc. **116**, 944 (1994).

[15] E. S. Pysh and N. C. Yang, J. Am. Chem. Soc. **85**, 2124 (1963).

[16] D. Rosseinsky and P. Kathirgamanathan, J. Chem. Soc. Perkin Trans. II, 135 (1985).

[17] A. K. Rappe, C. J. Casewit, K. S. Colwell, W. A. Goddard III, and W. M. Skiff, J. Am. Chem. Soc. **114**, 10 024 (1992).

[18] H. Reiss, J. Appl. Phys. **39**, 5045 (1968).

[19] F. C. Frank and J. H. van der Merwe, Proc. R. Soc. London Ser. A **198**, 205 (1949); J. H. van der Merwe, J. Appl. Phys. **41**, 4725 (1970).

[20] A. I. Kitaigorodsky, *Molecular Crystals and Molecules* (Academic, New York, 1973).

[21] N. L. Allinger, J. Am. Chem. Soc. **99**, 8127 (1977); J. T. Sprague, J. C. Tai, Y. Yuh, and N. L. Allinger, J. Comput. Chem. **8**, 581 (1987); S. J. Weiner, P. A. Kollman, D. A. Case, U. C. Singh, C. Ghio, G. Algona, S. Profeta, Jr., and P. Weiner, J. Am. Chem. Soc. **106**, 765 (1984); S. J. Weiner, P. A. Kollmann, D. T. Nguyen, and D. A. Case, J. Comput. Chem. **7**, 230 (1986); B. R. Brooks, R. E. Bruccoleri, B. D. Olafson, D. J. States, S. Swaminathan, and M. Karplus, J. Comput. Chem. **4**, 187 (1983); L. Nillson and M. Karplus, *ibid*. **7**, 591 (1986).

[22] A. Rappe, C. Casewit, K. Colwell, W. Goddard, and W. Skiff, J. Am. Chem. Soc. **114**, 10 024 (1992).

[23] S. Mayo, B. Olafson, and W. Goddard, J. Phys. Chem. **94**, 8897 (1990).

[24] J. H. van der Merwe, Philos. Mag. A **45**, 127 (1982).

[25] F. C. Frank and J. H. van der Merwe, Proc. R. Soc. London Ser. A **198**, 216 (1949); J. H. van der Merwe, Philos. Mag. A **45**, 145 (1982); J. H. van der Merwe, *ibid*. **45**, 159 (1982); H. Reiss, J. Appl. Phys. **39**, 5045 (1968); A. D. Novaco and J. P. MacTague, Phys. Rev. Lett. **38**, 1286 (1977); A. D. Novaco and J. P. McTague, Phys. Rev. B **19**, 5299 (1979).

[26] M. L. Anderson, V. S. Williams, T. J. Schuerlein, G. E. Collins, C. D. England, L.-K. Chau, P. A. Lee, K. W. Nebesny, and N. R. Armstrong, Surf. Sci. **307-309**, 551 (1994).

[27] E. Haskal, F. So, P. Burrows, and S. Forrest, Appl. Phys. Lett. **60**, 3223 (1992); S. R. Forrest, P. E. Burrows, E. I. Haskal, and Y. Zhang, in *Electrical, Optical, and Magnetic Properties of Organic Solid State Materials*, edited by A. F. Ganto, A. K.-Y. Jen, C. Y-C. Lee, and L. R. Dalton, MRS Symposia Proceedings, No. 328 (Materials Research Society, Pittsburgh, 1999); P. E. Burrows, Y. Zhang, I. Haskal, and S. R. Forrest, Appl. Phys. Lett. **61**, 2417 (1992).

[28] T. J. Schuerlein and N. R. Armstrong, J. Vac. Sci. Technol. A **12**, 1992 (1994).

[29] C. Ludwig, R. Strohmaier, J. Peterson, B. Gompf, and W. Eisenmenger, J. Vac. Sci. Technol. B **12**, 1963 (1994).

[30] J. C. Bucholz and G. A. Somorjai, J. Chem. Phys. **66**, 573 (1977).

[31] J. Hossick-Schott and M. D. Ward, J. Am. Chem. Soc. **116**, 6806 (1994); A. C. Hillier, J. Hossick-Schott, and M. D. Ward, Adv. Mater. **7**, 409 (1995).

[32] J. M. Williams, J. R. Ferraro, R. J. Thorn, K. D. Carlson, U. Geiser, H. H. Wang, A. M. Kini and M.-H. Whangbo, *Organic Superconductors* (Prentice Hall, Englewood Cliffs, NJ, 1992).

[33] The structure of $(Pe)_2ClO_4$ was assumed to be similar to that of $(Pe)_2PF_6$, which crystallize in the $P2/m$ space group with $a=13.04$ Å, $b=14.12$ Å, $c=13.75$ Å, and $\beta=110.8°$; H. Endres, H. K. Muller, and D. Schweitzer, Acta Crystallogr. C **41**, 607 (1985): H. Keller, D. Nothe, H. Pritzkow, D. Wehe, and M. Werner, Mol. Cryst. Liq. Cryst. **62**, 181 (1980). Other polymorphs examined for epitaxy were $(Pe)_3ClO_4$, which crystallizes in the $P1$ space group with $a=13.01$ Å, $b=13.82$ Å, $c=13.85$ Å, $\alpha=66.05°$, $\beta=83.36°$, and $\gamma=63.51°$; and Pe_6ClO_4 which crystallizes in the $P1$ space group with $a=12.571$ Å, $b=13.699$ Å, $c=13.835$ Å, $\alpha=110.43°$, $\beta=107.13°$, and $\gamma=107.09°$; H. Endres, H. K. Muller, and D. Schweitzer, Acta Crystallogr. C **41**, 607 (1985).

[34] (TTF)(TCNQ) crystallizes in the $P2_1/c$ space group, with $a=12.298$ Å, $b=3.819$ Å, $c=18.468$ Å, and $\beta=104.46°$; see T. J. Kistenmacher, T. E. Philipps, and D. O. Cowan, Acta Crystallogr. B **30**, 763 (1973).

[35] Due to the absence of a single-crystal structure for $(Pe)_2ClO_4$, the structure of $(Pe)_2PF_6$ salt was used for these analyses, but $(Pe)_2ClO_4$ was chosen for our experiments as its formation was better behaved than other salts.